Bismuth(III) - Thiophenedicarboxylates as Host Frameworks for Lanthanide Ions: Synthesis, Structural Characterization, and Photoluminescence

Alyssa K. Adcock,[1] *Bradley Gibbons,*[2] *Jeffrey D. Einkauf,*[3] *Jeffery A. Bertke,*[1] *J. Faye Rubinson,*[1] *Daniel T. de Lill,*[3] *and Karah E. Knope**[1]

[1]Department of Chemistry, Georgetown University, 37th and O Sts., NW, Washington, DC 20057
[2]Westminster College, 319 South Market Street, New Wilmington, PA 16172
[3]Department of Chemistry, Florida Atlantic University, 777 Glades Road, Boca Raton, FL 33431

Supporting Information

Crystallographic Refinement Details

Hpyr[Bi(TDC)$_2$(H$_2$O)]·1.5H$_2$O (1)

The coordinated water molecule, O30, is disordered over two positions. The Bi-O distances were restrained to be similar and similar displacement amplitudes were imposed on the disordered sites. One fully occupied water molecule, O40, and one partially occupied water molecule, O41, are present in the lattice. The site occupancy of O41 refines to approximately 50%. All pyridinium and water hydrogen atoms were located in the difference map. The N-H and O-H distances were restrained to be 0.88(2) Å. Remaining H atoms were included as riding idealized contributors. Water and pyridinium H atom U's were assigned as 1.5 times U_{eq} of the carrier atom; remaining H atom U's were assigned as 1.2 times carrier U_{eq}.

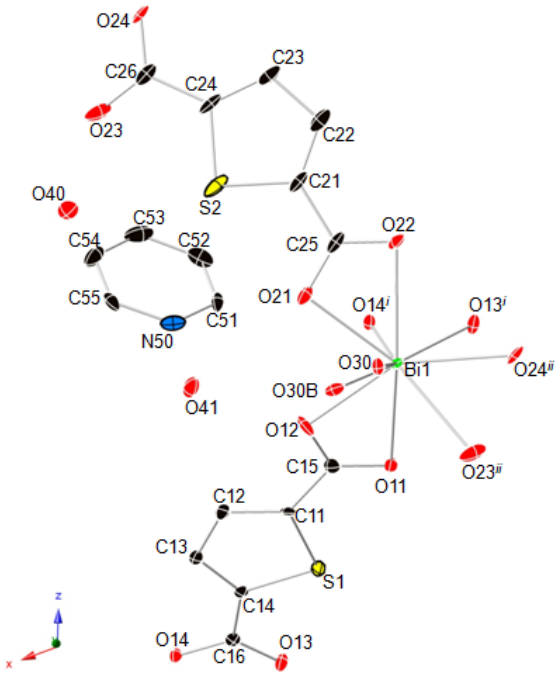

Figure S1. Thermal ellipsoid plot of **1**. Ellipsoids are shown at 50% probability. Symmetry codes: (i) x - 1/2, -y + 3/2, z + 1/2; (ii) x - 1, y, z - 1.

[Hpy]$_3$[Bi$_2$(TDC)$_4$(HTDC)(H$_2$O)]·xH$_2$O (2)

Due to crystallographic challenges primarily concerning disorder of one of the pyridinium rings, only a preliminary structure refinement has been determined. Multiple datasets were collected, and the best of these is presented here. One pyridinium cation is disordered over two positions. Another cation is disordered over three orientations and across a symmetry site. One positions has been constrained to 50% occupancy, while the other two orientations were freely refined with the sum of their occupancies set to 50%. All three orientations were constrained to be perfect

hexagons. The carboxylate moiety of one TDC ligand is disordered over two positions. The like O-C distances were restrained to be similar. O24 was restrained to behave relatively isotropic. The coordinated water molecule is disordered over two sites. The Bi-O distances were restrained to be similar. Similar displacement amplitudes were imposed on all the disordered sites overlapping by less than the sum of van der Waals radii. The H atoms for the water molecules could not be located in the difference map and thus were left out of the model. The pyridinium N-H and hydroxyl O-H hydrogen atoms also could not be located in the difference map and were placed in calculated positions. Remaining H atoms were included as riding idealized contributors. Hydroxyl H atom U's were assigned as 1.5 times U_{eq} of the carrier atom; remaining H atom U's were assigned as 1.2 times carrier U_{eq}.

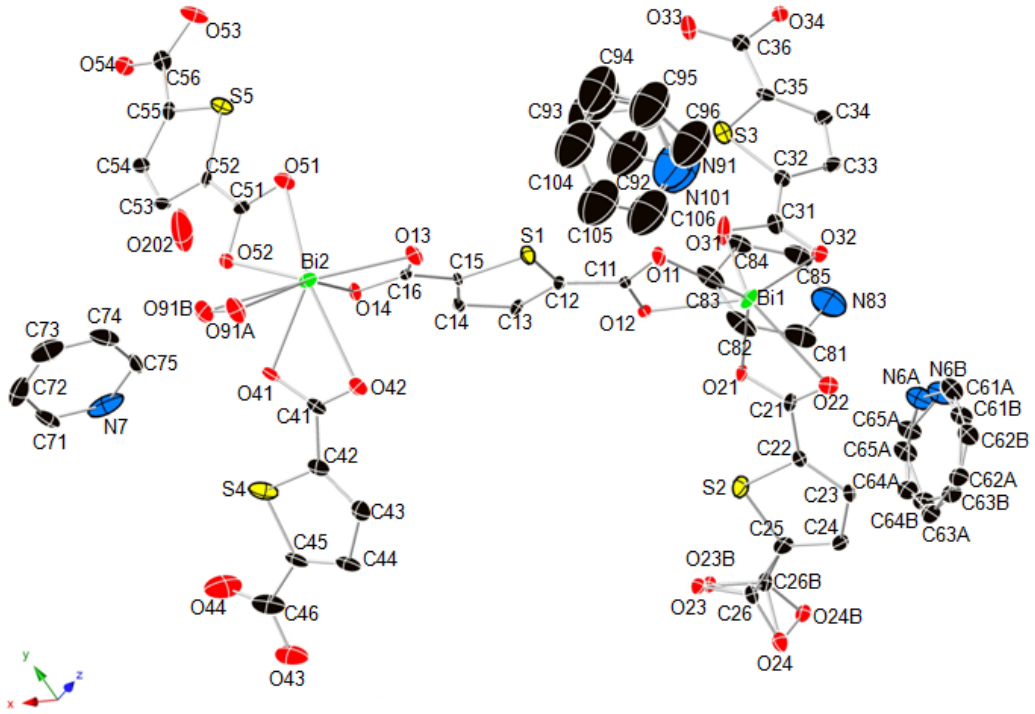

Figure S2. Thermal ellipsoid plot of **2**. Ellipsoids are shown at 50% probability. Symmetry codes: (i) x - 1, y + 1, z; (ii) x - 1, y - 1, z.

$(Hpyr)_2[Bi(TDC)_2(HTDC)]\cdot 0.36H_2O$ (3)

One carboxylate group of a TDC ligand is disordered over two positions. The like O-C and C-C distances were restrained to be similar. Both pyridinium cations are disordered over two positions; one is disordered about a symmetry site. The rings were constrained to be perfect hexagons. Similar displacement amplitudes were imposed on the disordered sites overlapping by less than the sum of van der Waals radii. A partially occupied lattice water molecule, O61, is present and the site occupancy refines to approximately 36%. The hydrogen atoms of the partially occupied water molecule could not be located in the difference map and thus were left out of the model.

The hydroxyl hydrogen atom of the HTDC ligand was located in the difference map and the O-H distance was restrained to be 0.88(2) Å. Remaining H atoms were included as riding idealized contributors. Hydroxyl H atom U's were assigned as 1.5 times U_{eq} of the carrier atom; remaining H atom U's were assigned as 1.2 times carrier U_{eq}.

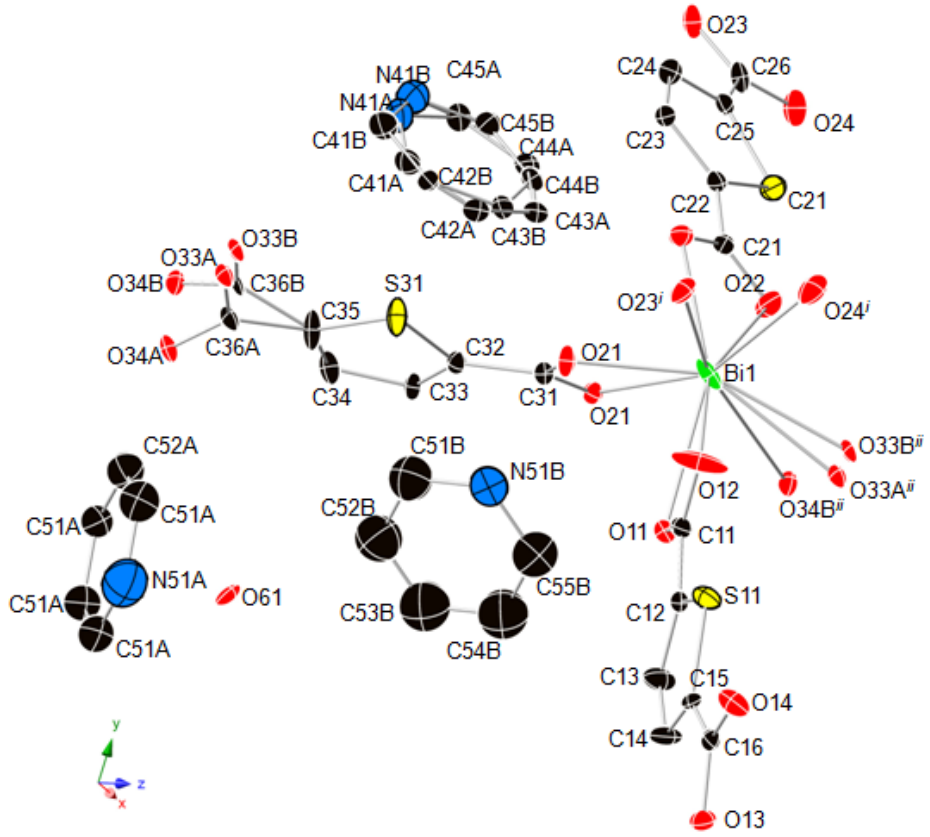

Figure S3. Thermal ellipsoid plot of **3**. Ellipsoids are shown at 50% probability. Symmetry codes: (i) x - 1/2, -y + 3/2, z + 1/2; (ii) x + 1, y, z + 1.

Eu(TDC)(NO_3)(H_2O) (4)

The refinement was processed as a two component twin, although only the first domain was used for the subsequent refinement. Non-overlapping reflections from the primary orientation were used for phasing and refinement. Due to the high amount of overlap in both domains, inclusion of the minor orientation resulted in a less reliable model. The primary orientation still contains over 99% completeness, thus a reliable model could be determined from only the first domain. Several reflections were omitted from the final refinement. The water H atoms were located in the difference map and the O-H distances were restrained to be 0.88(2) Å. Remaining H atoms were included as riding idealized contributors. Water H atom U's were assigned as 1.5 times U_{eq} of the carrier atom; remaining H atom U's were assigned as 1.2 times carrier U_{eq}.

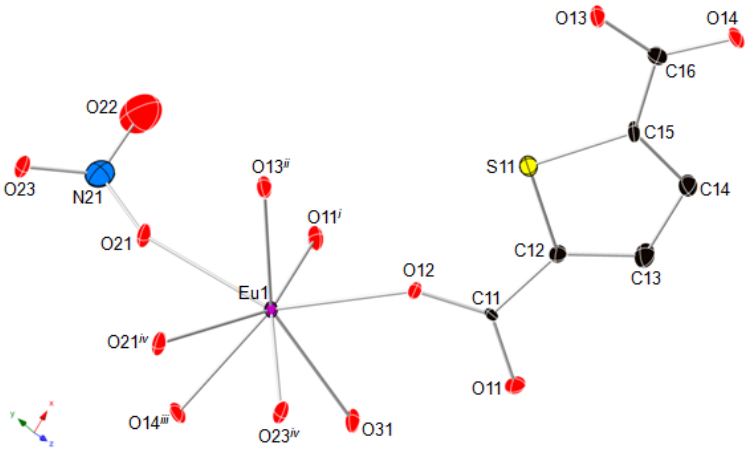

Figure S4. Thermal ellipsoid plot of **4**. Ellipsoids are shown at 50% probability. Symmetry codes: (i) x, -y+1/2, z-1/2, (ii) -x+1, -y+1, -z+1, (iii) x-1, y, z-1, (iv) -x, -y+1, -z.

$[Eu_2(TDC)3(H_2O)_9]\cdot 5H_2O$ (5)

The atoms of the TDC ligands were restrained to behave relatively isotropic. Three of the carboxylate carbon atoms (C11, C21, and C26) were constrained to have equal anisotropic displacement parameters. Rigid body restraints were imposed on all atoms. One reflection was omitted from the final refinement. The water H atoms (bound and solvent) could not be located in the difference map and thus were left out of the model. Remaining H atoms were included as riding idealized contributors. H atom U's were assigned as 1.2 times carrier U_{eq}.

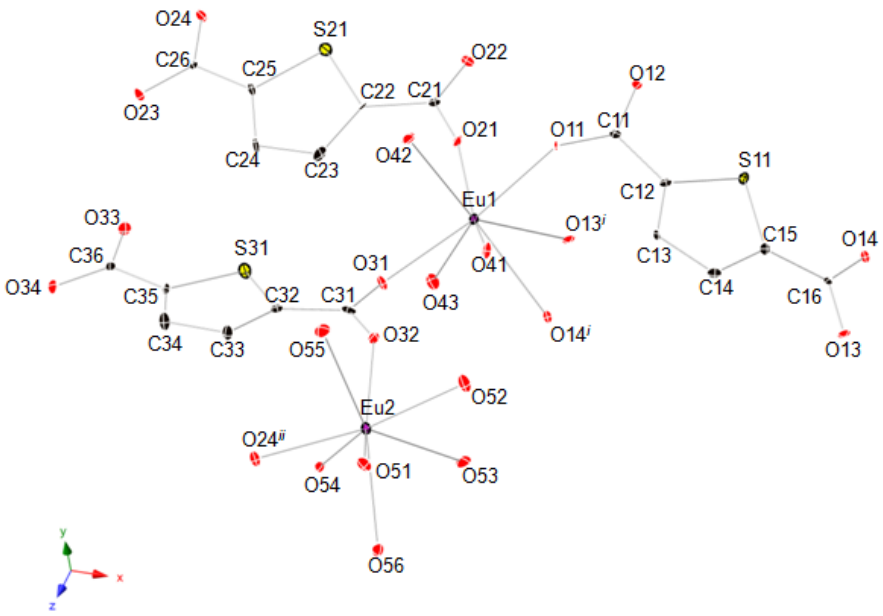

Figure S5. Thermal ellipsoid plot of **5**. Ellipsoids are shown at 50% probability. Symmetry codes: (i) -x + 1, -y, -z + 1; (ii) -x + 1/2, -y + 1/2, z + 1/2.

Powder X-Ray Diffraction

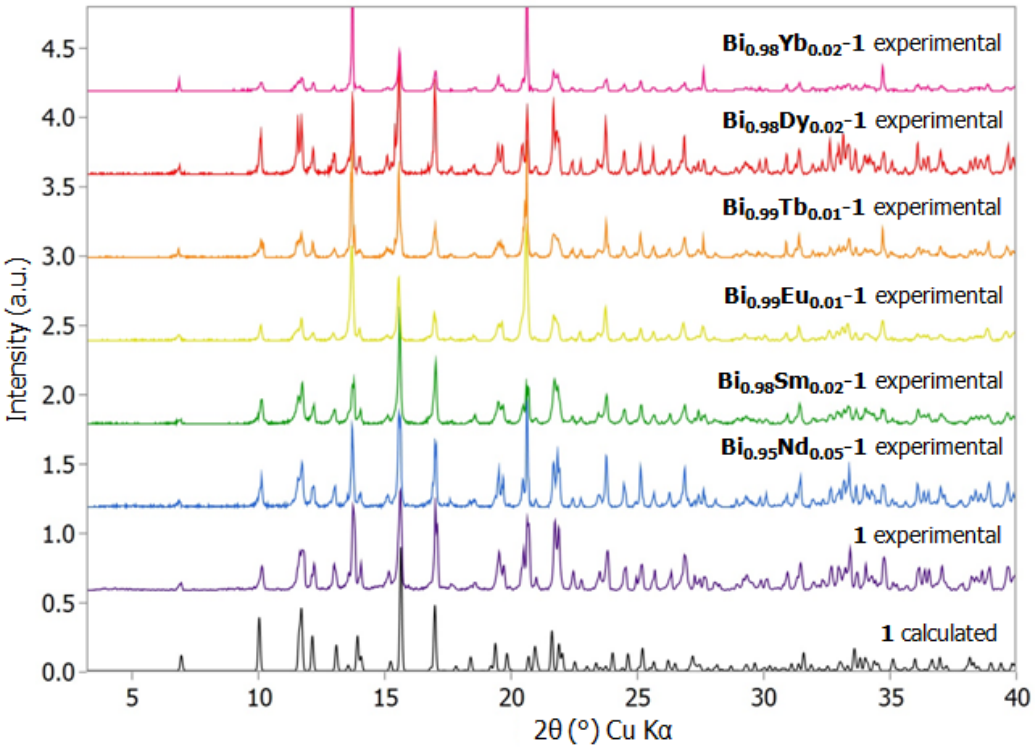

Figure S6. Powder X-ray diffraction data for the bulk product from which **1** and $\mathbf{Bi_{1-x}Ln_x}$**-1** (Ln=Nd, Sm, Eu, Tb, Dy, and Yb) were isolated. Agreement between the calculated pattern generated from the crystallographic information file and the experimental data support that the crystal used for structure determination is representative of the bulk.

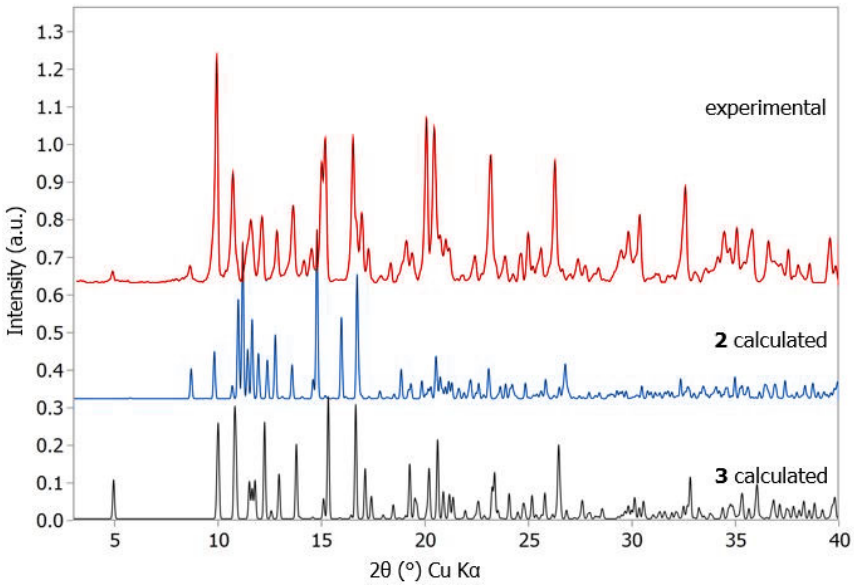

Figure S7. Powder X-ray diffraction data for the bulk product from which **2** and **3** were isolated. The calculated patterns generated from the crystallographic information files of **2** and **3** are overlaid with the experimental pattern.

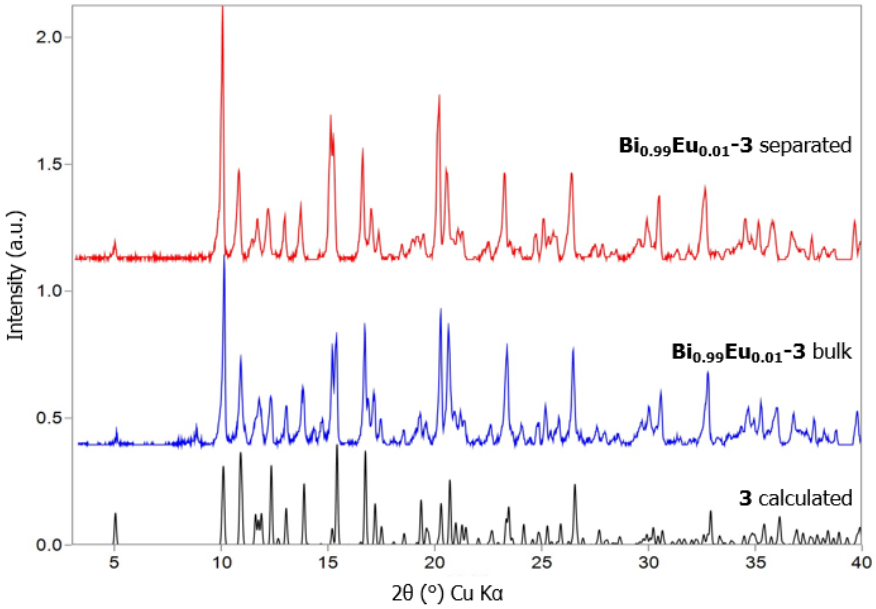

Figure S8. Powder X-ray diffraction data for the bulk product from which **$Bi_{0.99}Eu_{0.01}$-3** was isolated both before and after manual separation. Agreement between the calculated pattern generated from the CIF and the experimental data support phase purity of the manually separated sample of **$Bi_{0.99}Eu_{0.01}$-3.**

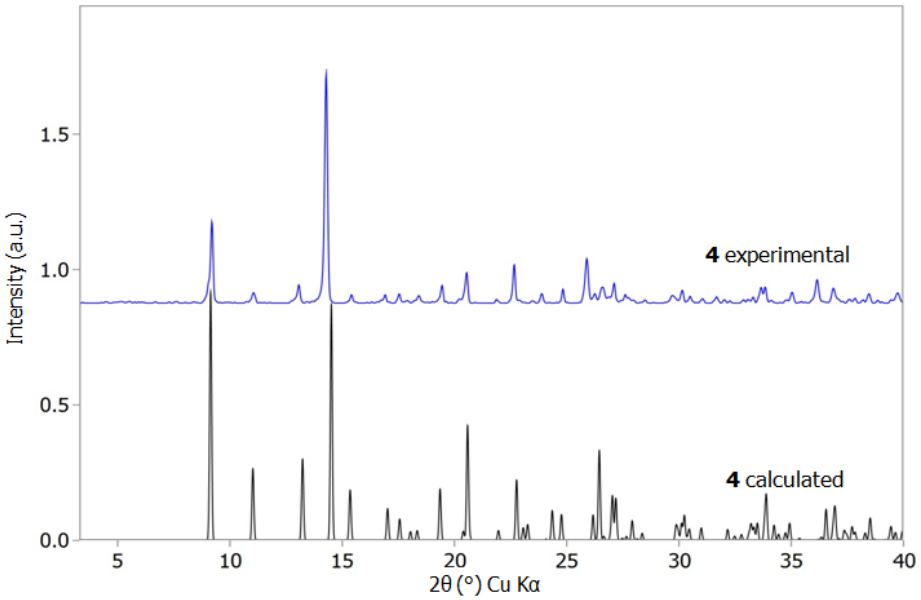

Figure S9. Powder X-ray diffraction data for the bulk product from which **4** was isolated. Agreement between the calculated pattern generated from the crystallographic information file and the experimental data support that the single crystal used for structure determination is representative of the bulk; however, subsequent elemental analysis indicated the presence of a minor impurity not seen in by powder.

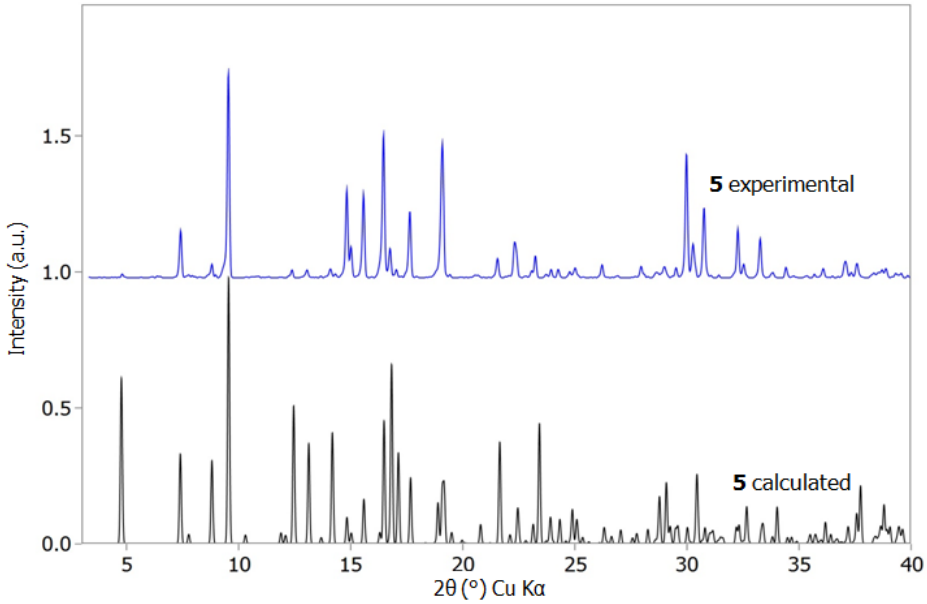

Figure S10. Powder X-ray diffraction data for the bulk product from which **5** was isolated. Agreement between the calculated pattern generated from the crystallographic information file and the experimental data support that the single crystal used for structure determination is representative of the bulk.

Raman Spectra

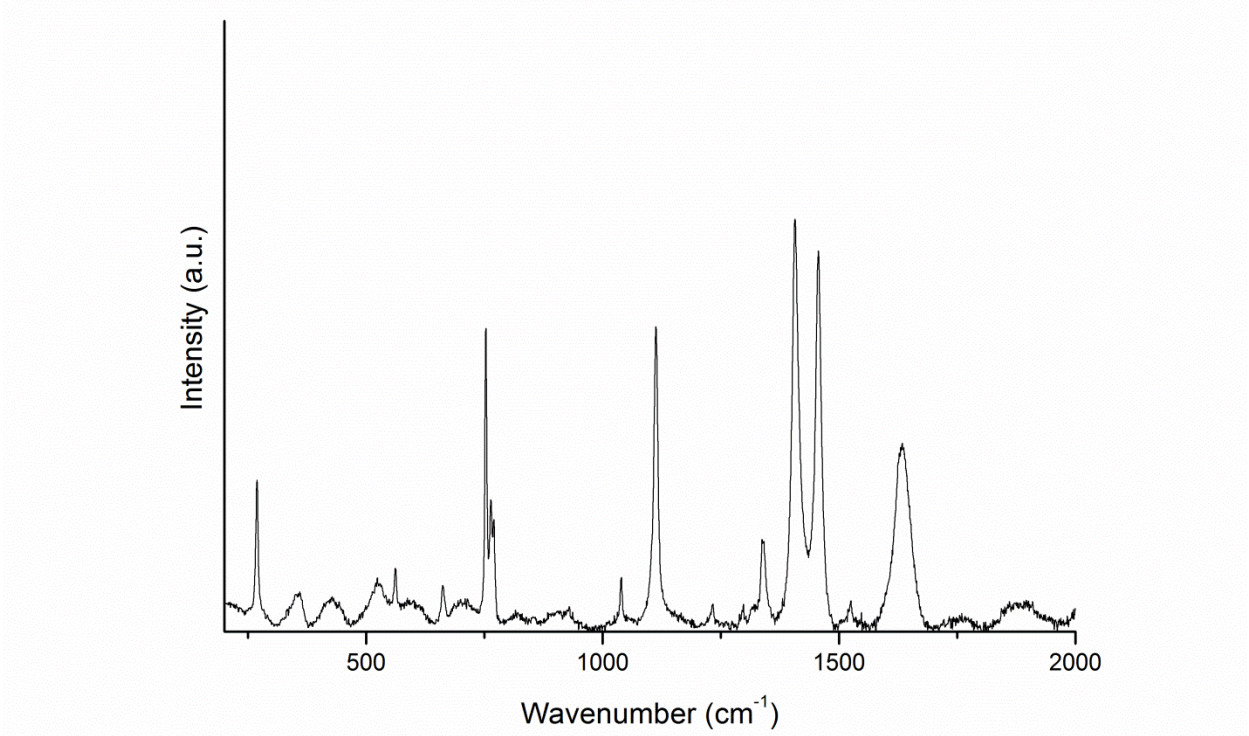

Figure S11. Raman spectrum for 2,5-thiophenedicarboxylic acid shown over 200-2000 cm^{-1}.

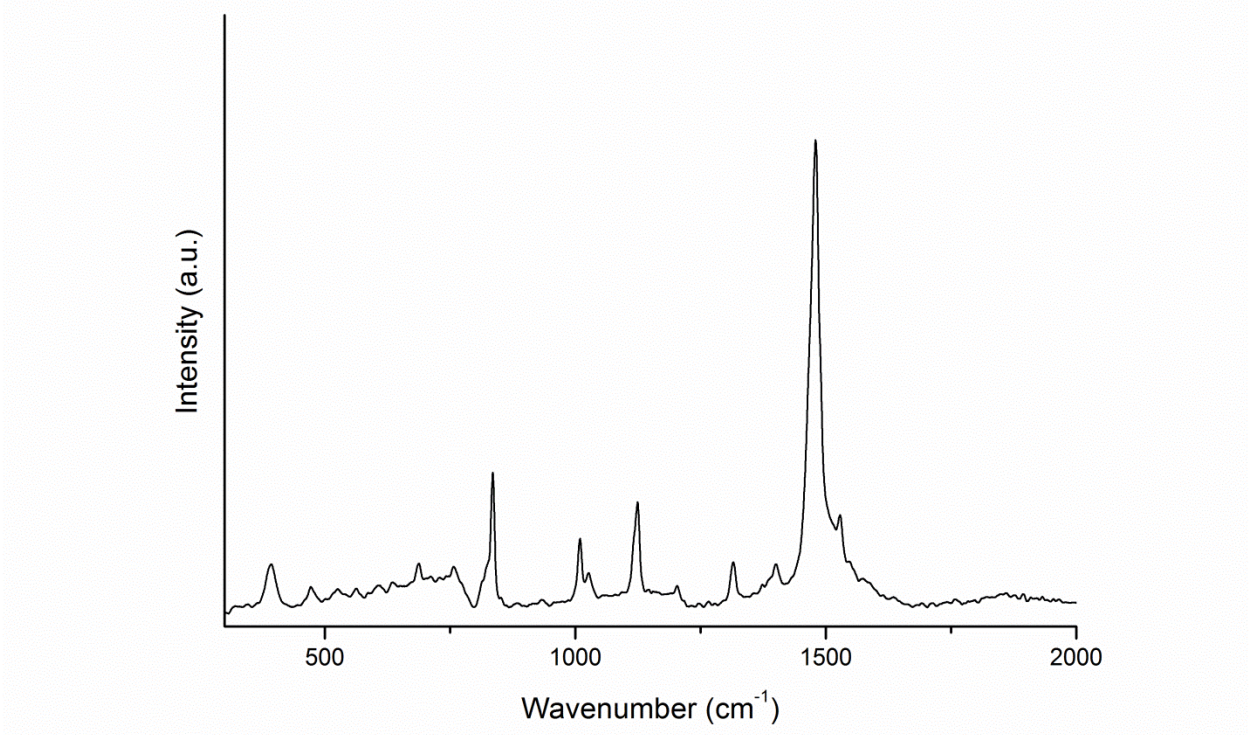

Figure S12. Raman spectrum for **1** shown over 200-2000 cm^{-1}.

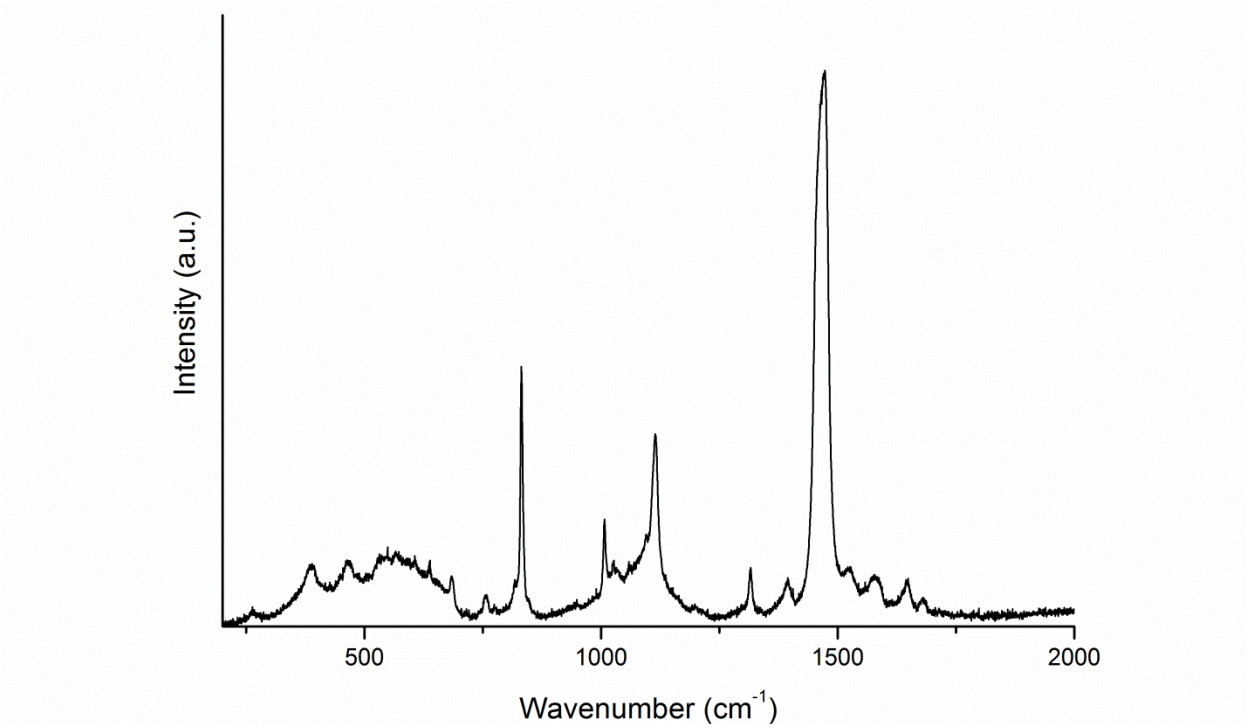

Figure S13. Raman spectrum for **2** shown over 200-2000 cm^{-1}.

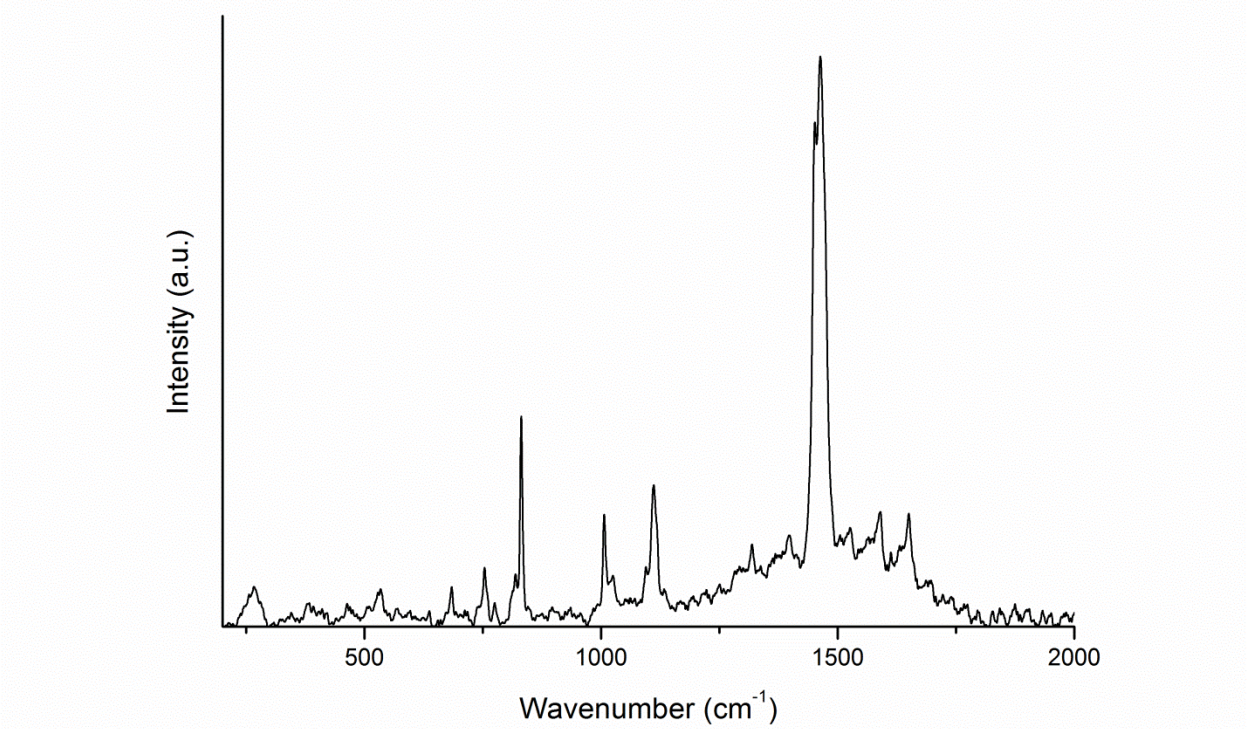

Figure S14. Raman spectrum for **3** shown over 200-2000 cm^{-1}.

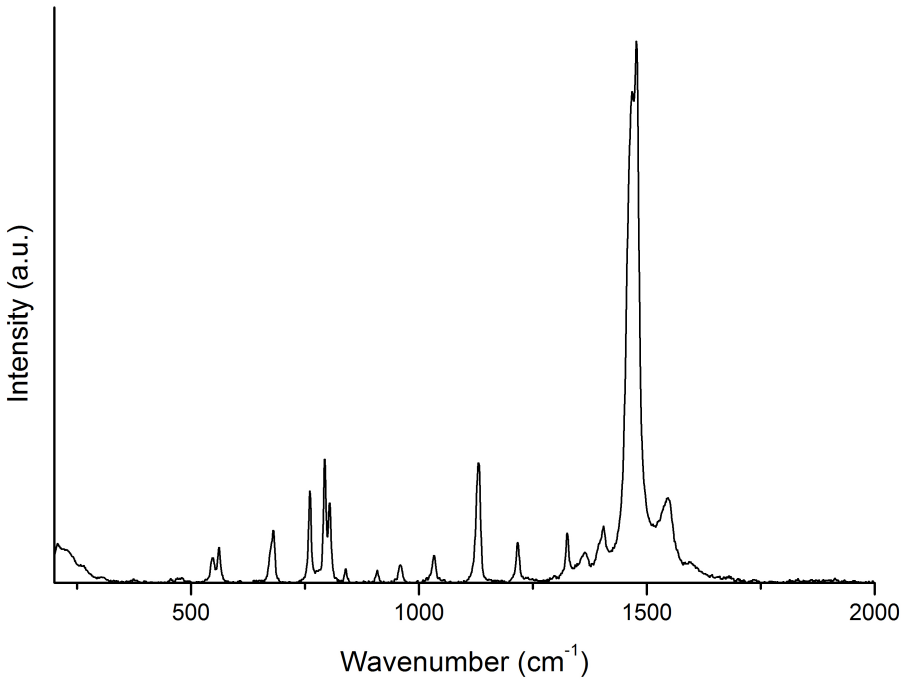

Figure S15. Raman spectrum for **4** shown over 200-2000 cm^{-1}.

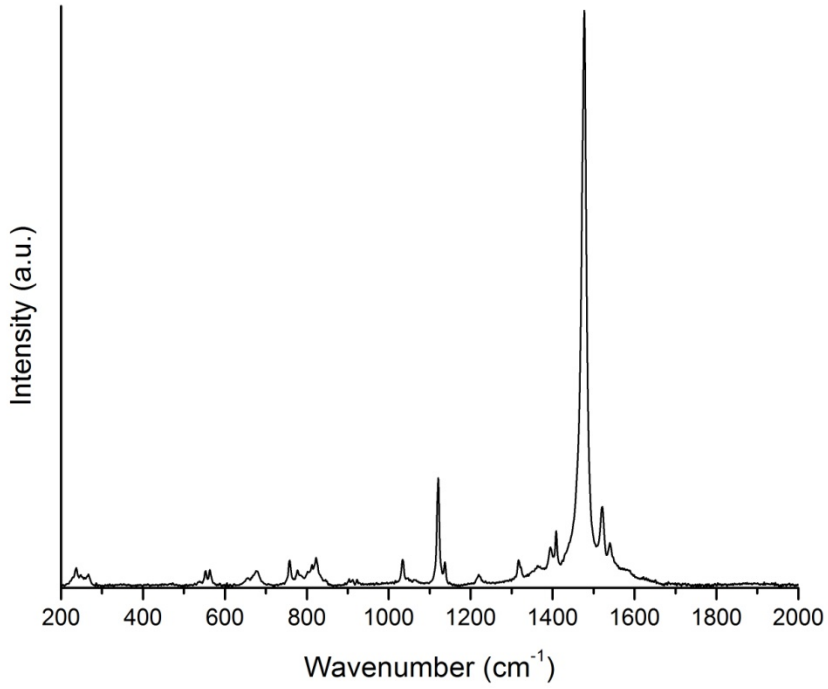

Figure S16. Raman spectrum for **5** shown over 200-2000 cm^{-1}.

Thermal Analysis

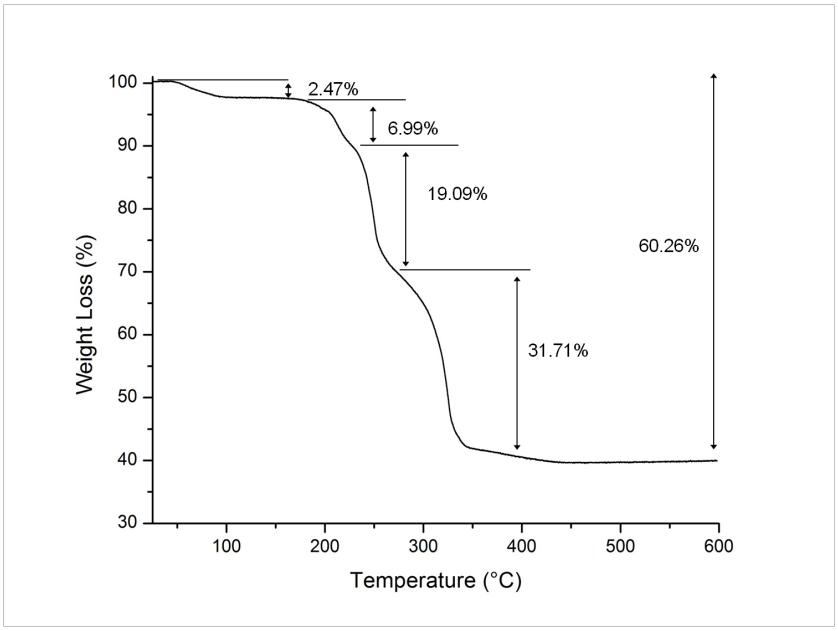

Figure S17. TGA plot for **1** collected over 25-600°C.

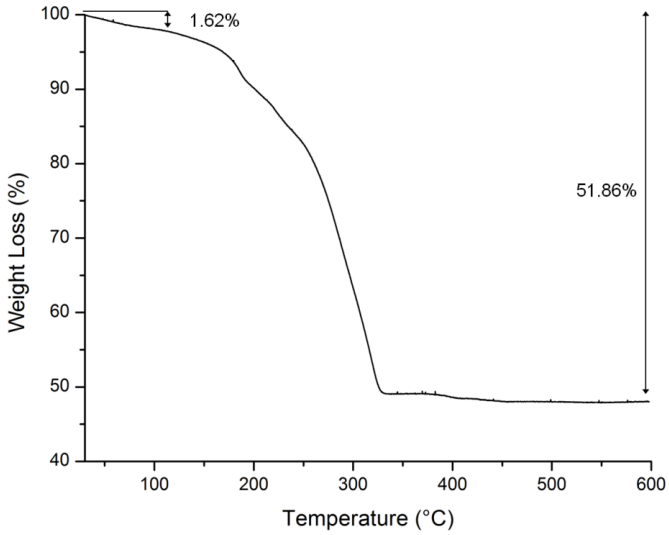

Figure S18. TGA plot for **$Bi_{0.99}Eu_{0.01}$-3** collected over 25-600°C.

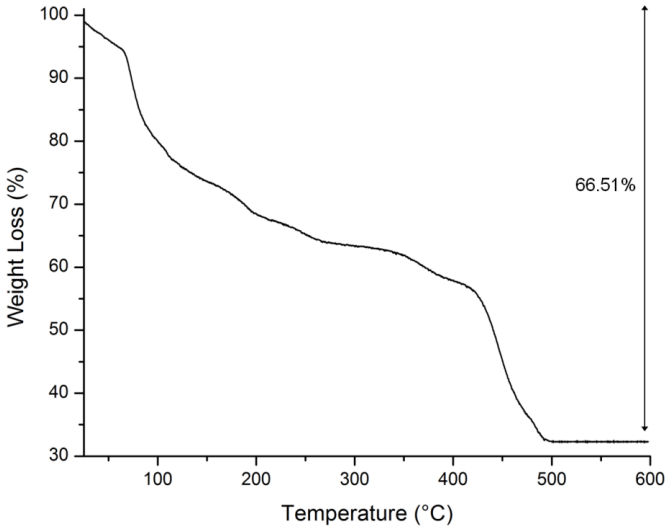

Figure S19. TGA plot for **5** collected over 25-600°C.

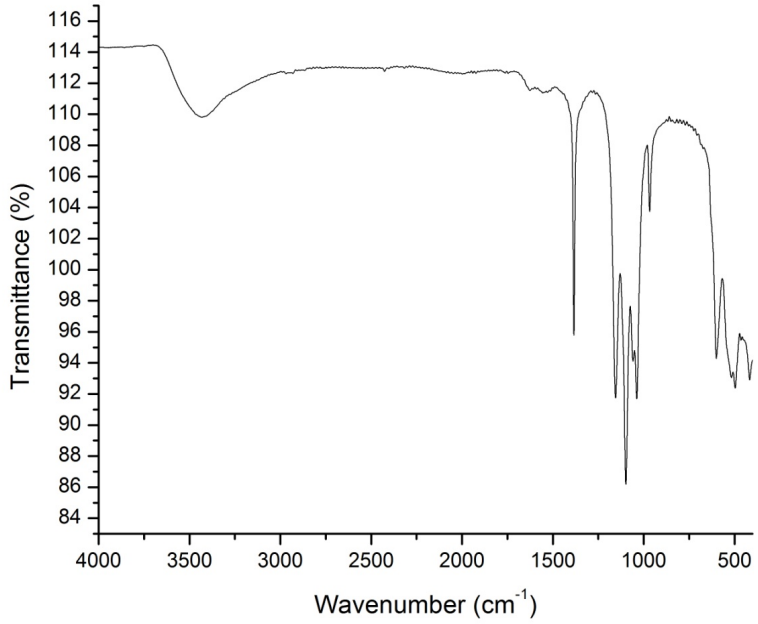

Figure S20. Infrared spectrum for the thermal decomposition product of **1**.

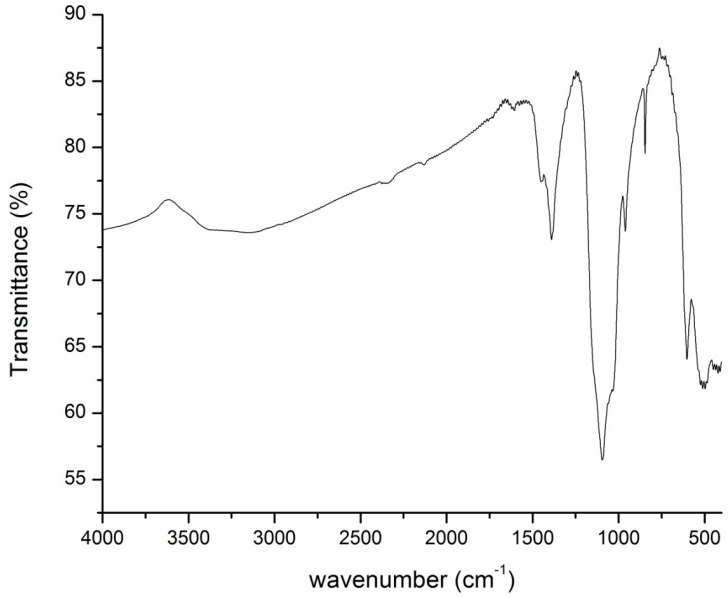

Figure S21. Infrared spectrum for the thermal decomposition product of **$Bi_{0.99}Eu_{0.01}$-3**.

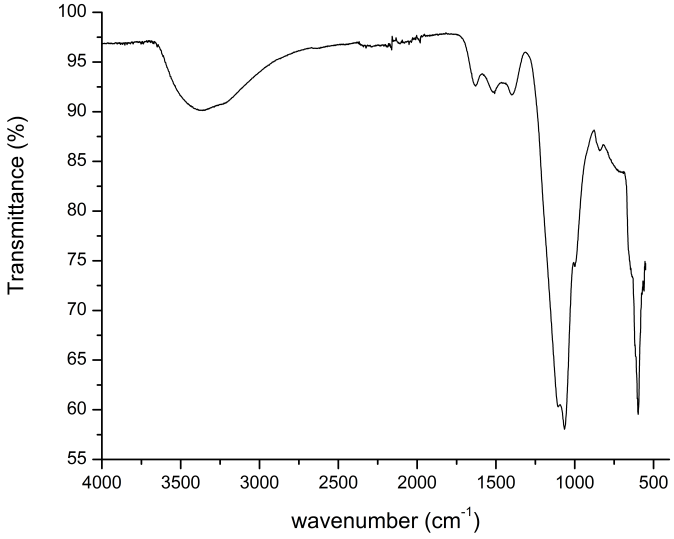

Figure S22. Infrared spectrum for the thermal decomposition product of **5**.

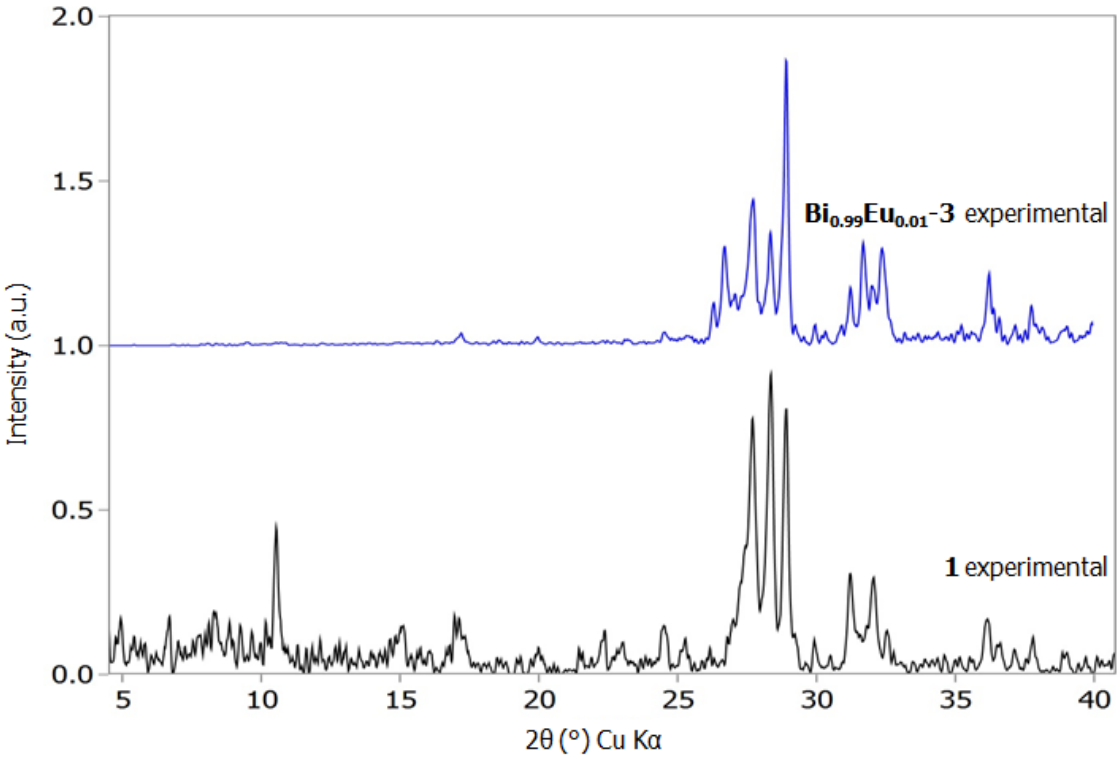

Figure S23. Powder X-ray diffraction data for the thermal decomposition products of **1** and **$Bi_{0.99}Eu_{0.01}$-3**. Attempts to index the peaks to a calculated phase proved unsuccessful.

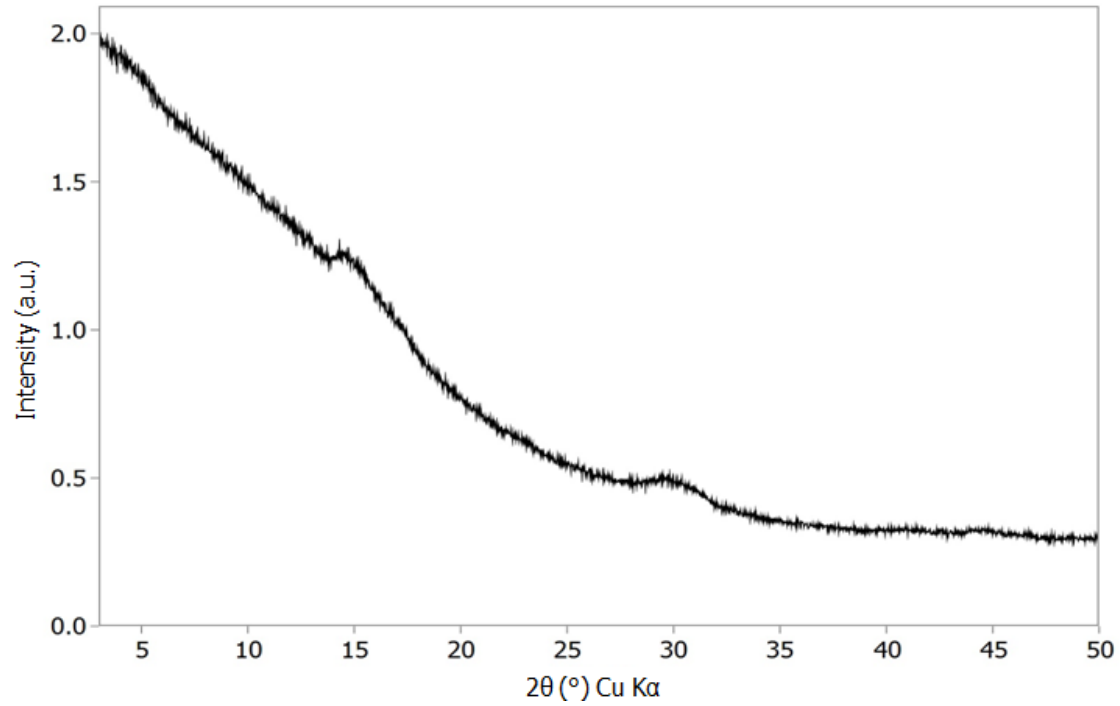

Figure S24. Powder X-ray diffraction data for the thermal decomposition product of **5.**

Luminescence Measurements

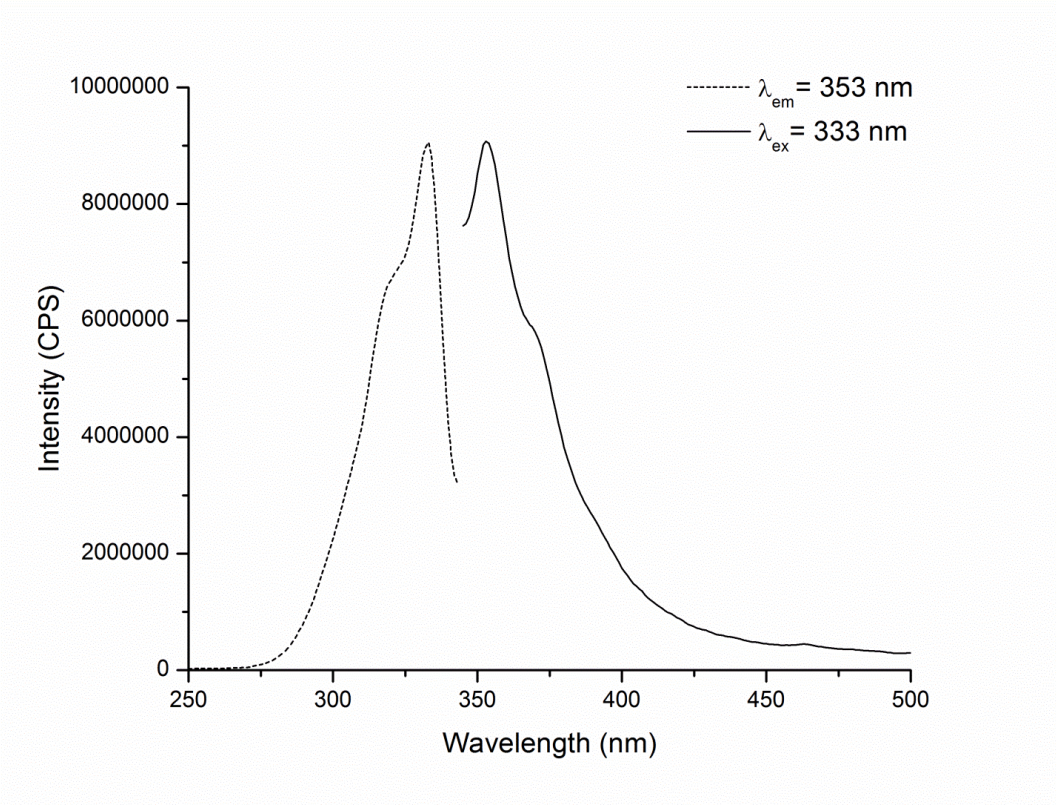

Figure S25. Excitation and emission spectra for 2,5-thiophenedicarboxylic acid.

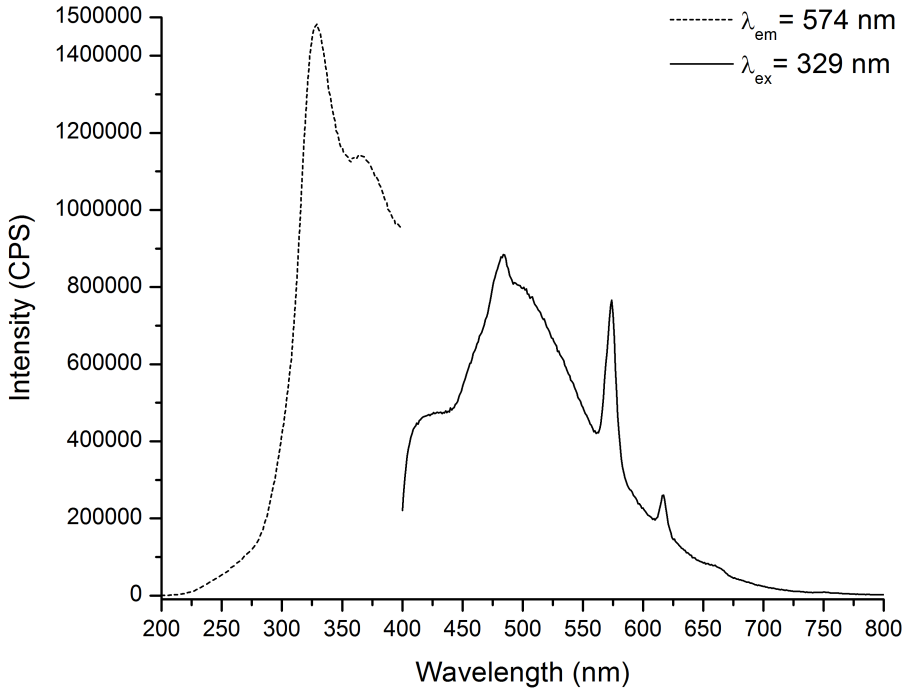

Figure S26. Excitation (dashed line) and emission (solid line) spectra for **$Bi_{0.98}Dy_{0.02}$-1** phase.

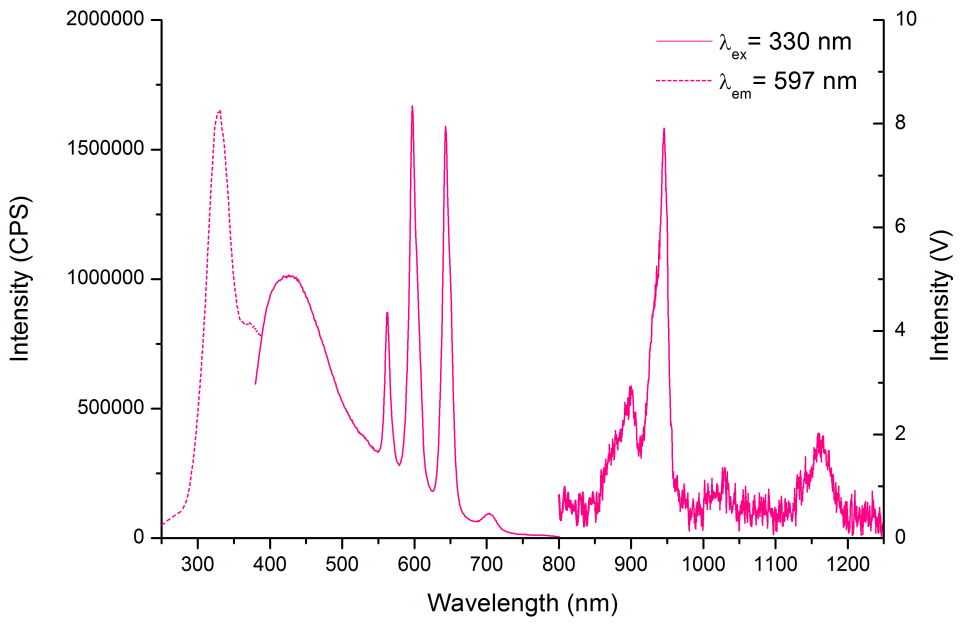

Figure S27. Excitation (dashed line) and emission (solid line) spectra for **$Bi_{0.98}Sm_{0.02}$-1**.

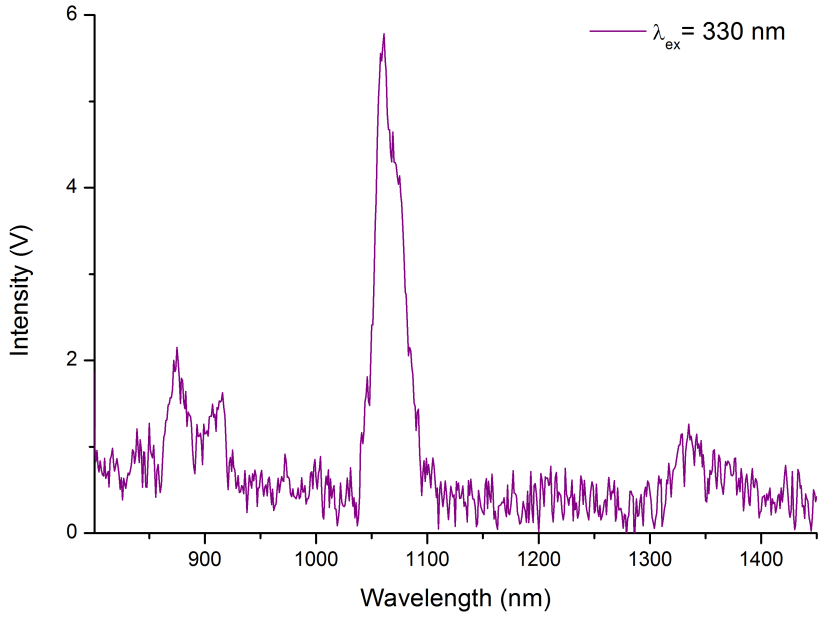

Figure S28. Emission spectrum for **$Bi_{0.95}Nd_{0.05}$-1**.

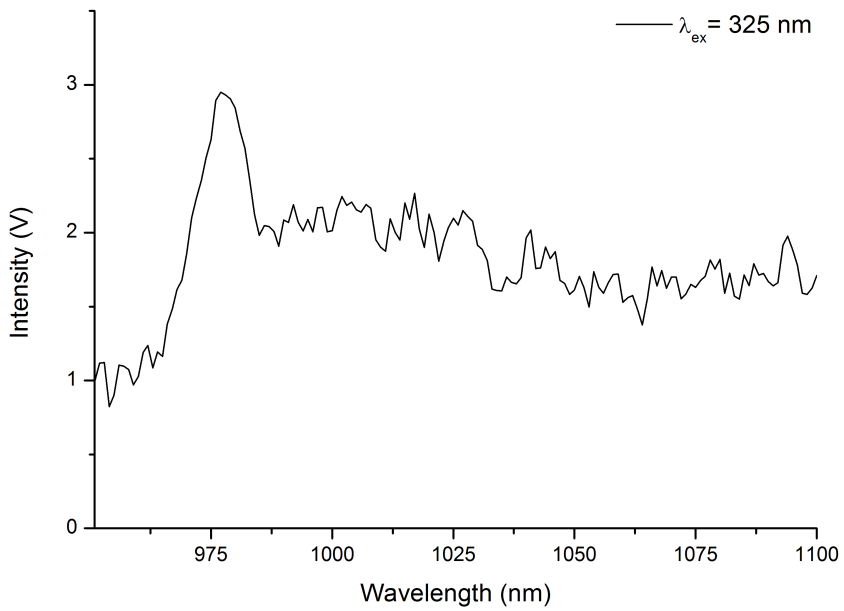

Figure S29. Emission spectrum for **$Bi_{0.98}Yb_{0.02}$-1**.

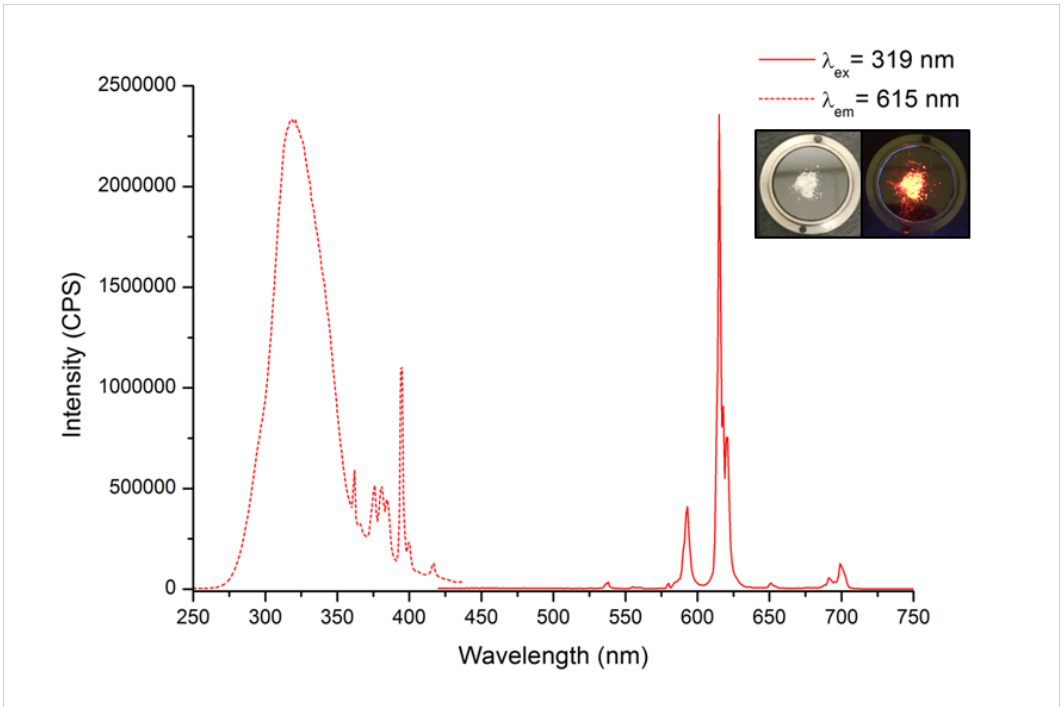

Figure S30. Excitation (dashed line) and emission (solid line) spectra for **5**. Inset depicts the bulk powder under ambient light (left) and UV irradiation from a handheld lamp (right).

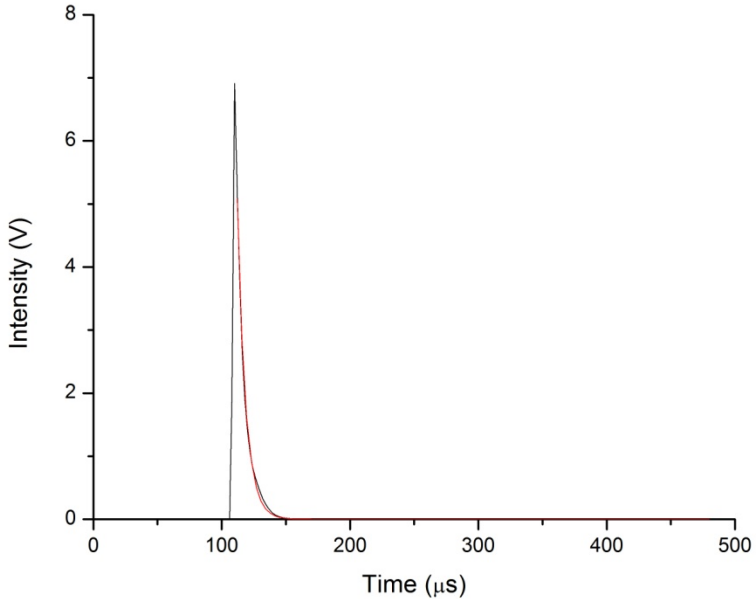

Figure S31. Lifetime decay curve for **1**, with the exponential decay fit plotted in red.

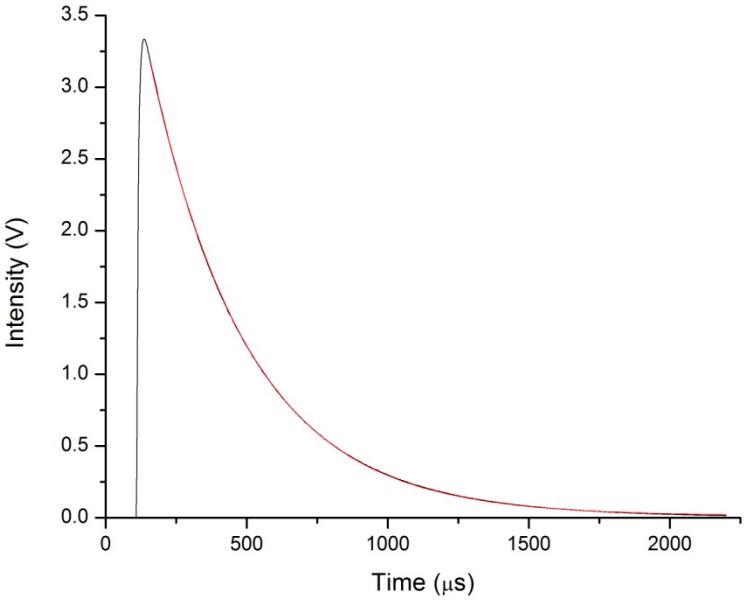

Figure S32. Lifetime decay curve for **$Bi_{0.99}Eu_{0.01}$-1**, with the exponential decay fit plotted in red.

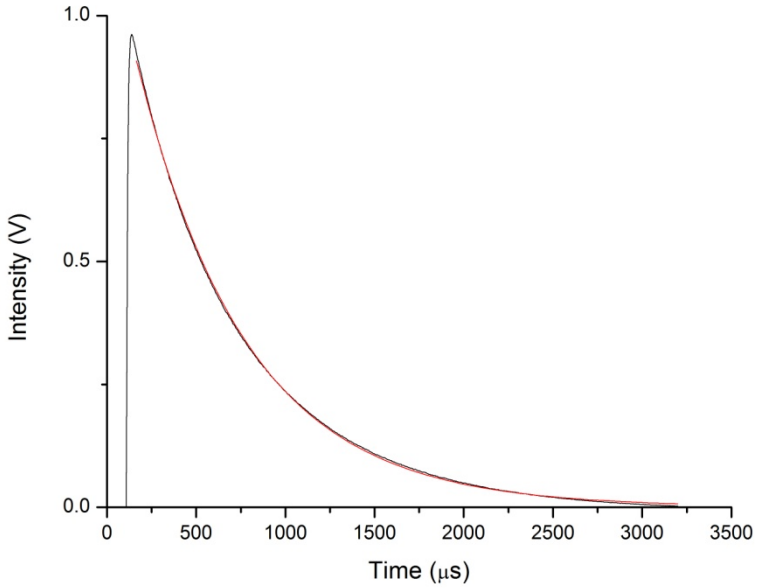

Figure S33. Lifetime decay curve for **$Bi_{0.99}Eu_{0.01}$-3**, with the exponential decay fit plotted in red.

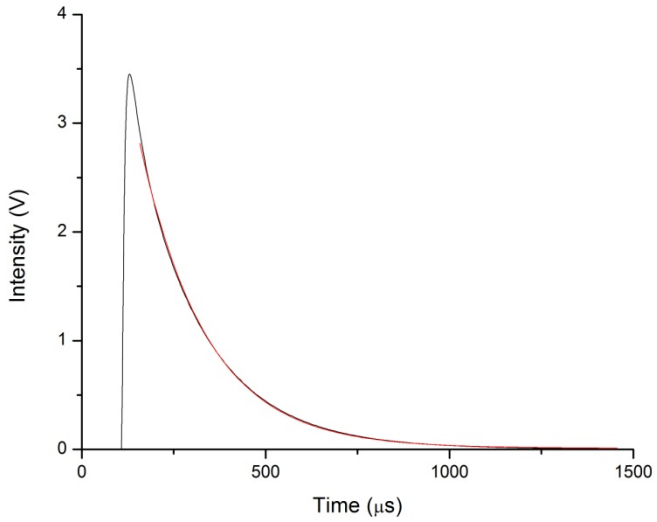

Figure S34. Lifetime decay curve for **5**, with the exponential decay fit plotted in red.

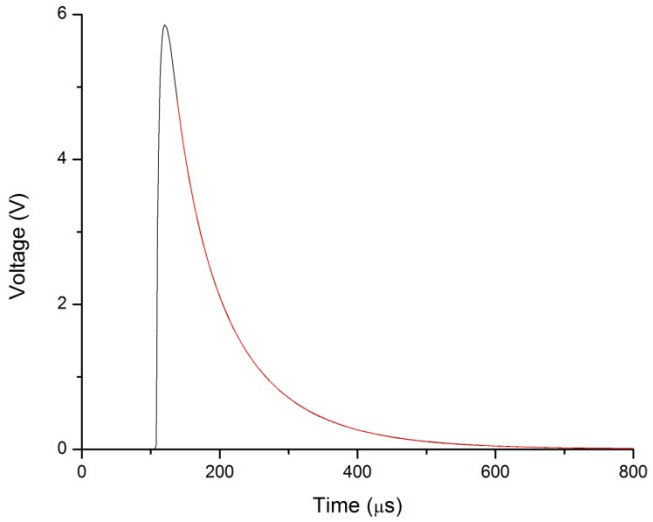

Figure S35. Lifetime decay curve for **$Bi_{0.99}Tb_{0.01}$-1**, with the exponential decay fit plotted in red.

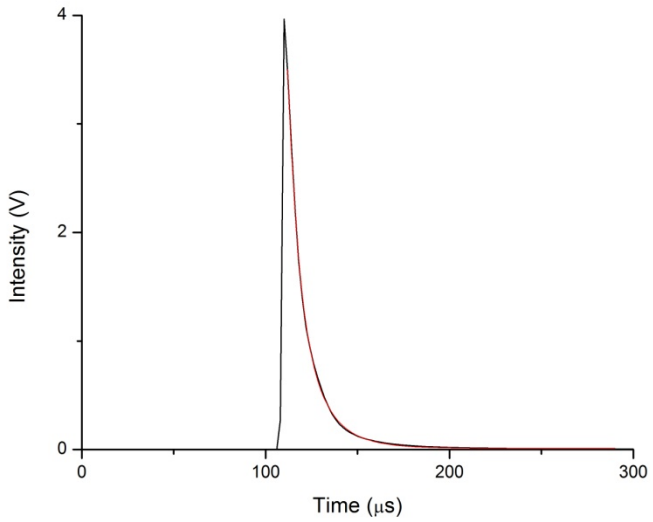

Figure S36. Lifetime decay curve for **$Bi_{0.98}Dy_{0.02}$-1**, with the exponential decay fit plotted in red.

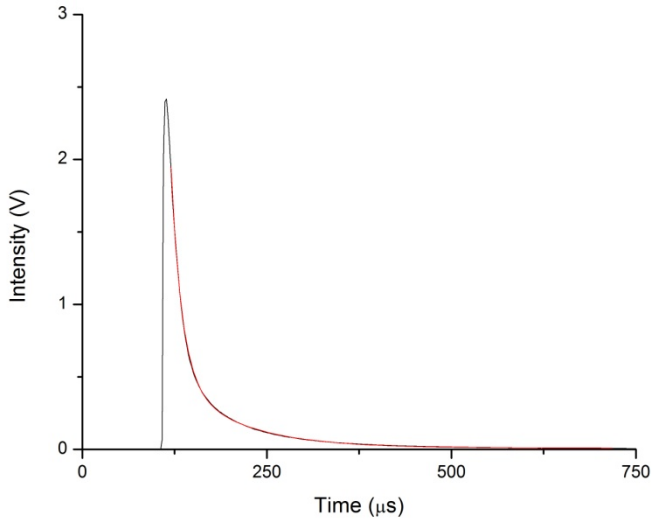

Figure S37. Lifetime decay curve for **$Bi_{0.98}Sm_{0.02}$-1**, with the exponential decay fit plotted in red.

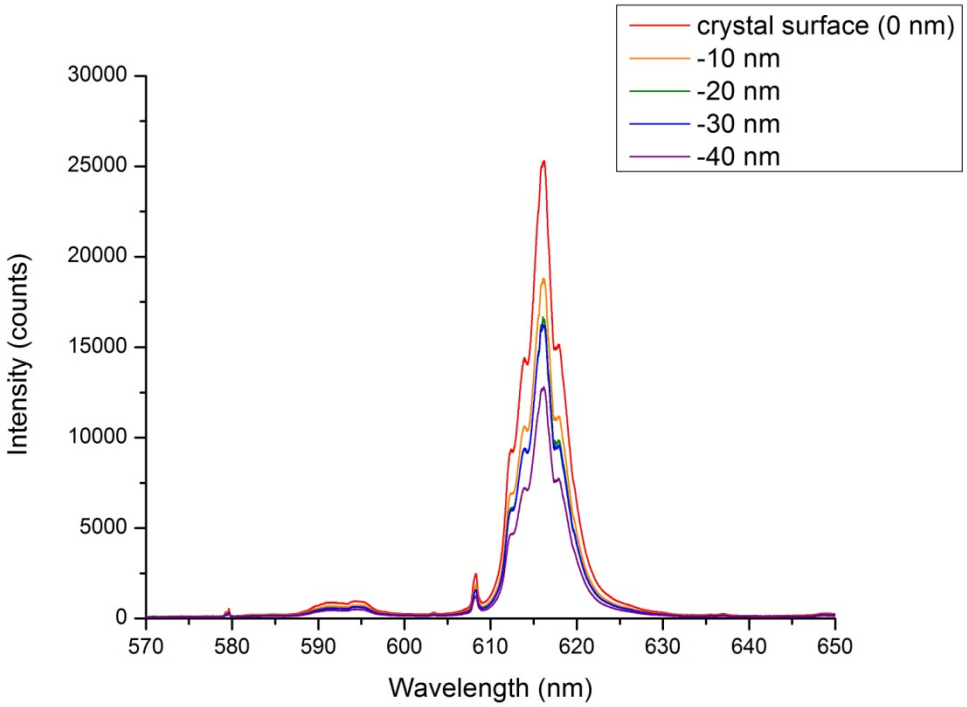

Figure S38. Raman luminescence spectra for **$Bi_{0.99}Eu_{0.01}$-1** plotted over 570 to 650 nm measured at varying depths of the crystal.